Biochemical and Biophysical Research Communications 381 (2009) 16–21

Contents lists available at ScienceDirect

Biochemical and Biophysical Research Communications

journal homepage: www.elsevier.com/locate/ybbrc

Crystal structure of the glycosidase family 73 peptidoglycan hydrolase FlgJ ☆

Wataru Hashimoto [a], Akihito Ochiai [a], Keiko Momma [a], Takafumi Itoh [a], Bunzo Mikami [b], Yukie Maruyama [a], Kousaku Murata [a,*]

[a] Laboratory of Basic and Applied Molecular Biotechnology, Graduate School of Agriculture, Kyoto University, Uji, Kyoto 611-0011, Japan
[b] Laboratory of Applied Structural Biology, Graduate School of Agriculture, Kyoto University, Uji, Kyoto 611-0011, Japan

ARTICLE INFO

Article history:
Received 20 January 2009
Available online 7 February 2009

Keywords:
Sphingomonas
Peptidoglycan
Glycoside hydrolase
FlgJ
Crystal structure

ABSTRACT

Glycoside hydrolase (GH) categorized into family 73 plays an important role in degrading bacterial cell wall peptidoglycan. The flagellar protein FlgJ contains N- and C-terminal domains responsible for flagellar rod assembly and peptidoglycan hydrolysis, respectively. A member of family GH-73, the C-terminal domain (SPH1045-C) of FlgJ from *Sphingomonas* sp. strain A1 was expressed in *Escherichia coli*, purified, and characterized. SPH1045-C exhibited bacterial cell lytic activity most efficiently at pH 6.0 and 37 °C. The X-ray crystallographic structure of SPH1045-C was determined at 1.74 Å resolution by single-wavelength anomalous diffraction. The enzyme consists of two lobes, α and β. A deep cleft located between the two lobes can accommodate polymer molecules, suggesting that the active site is located in the cleft. Although SPH1045-C shows a structural homology with family GH-22 and GH-23 lysozymes, the arrangement of the nucleophile/base residue in the active site is specific to each peptidoglycan hydrolase.

Peptidoglycan found in all bacteria plays an important role in protecting cells against physical and chemical stress, such as osmotic pressure [1]. A typical peptidoglycan consists of *N*-acetylglucosamine (GlcNAc) and *N*-acetylmuramic acid (MurNAc) as the main chain and a tetrapeptide attached to the C3 position of MurNAc [2]. The glycan includes a disaccharide-repeating unit [-MurNAc-(1->4)-β-D-GlcNAc-], and the bridge formation between the side peptide chains contributes to the strength and elasticity of the peptidoglycan layers.

Degradation of peptidoglycans in bacterial cells is involved in important cell activities, including metabolism and synthesis of the cell wall, differentiation and proliferation of cells, cell lysis, flagella formation, spore formation, and competency [3]. Several enzymes are responsible for degrading the glycan or peptide region as follows [4]: *N*-acetylglucosaminidase, *N*-acetylmuramidase, *N*-acetylmuramoyl-L-alanine amidase, D,L-endopeptidase, and transglycosidase. Glycan-degrading enzymes, especially lysozymes, are well characterized because hosts, including humans, possess cell lytic enzymes to protect against bacterial infection [5].

Polysaccharide-degrading enzymes are categorized into two groups: hydrolases and lyases. Glycoside hydrolases (GHs) are classified in the CAZy (Carbohydrate-Active enZyme) database into 114 families based on their primary structure [6,7], while polysaccharide lyases (PLs) are classified into 21 families. To understand the nature of enzyme catalysis and substrate recognition, we have comprehensively analyzed the structure and function of several polysaccharide-degrading enzymes, specifically families GH-78, GH-88, and GH-105, and PL-5, PL-7, PL-8, PL-11, PL-14, and PL-15 enzymes [8–10]. The GHs involved in degrading peptidoglycan are categorized into five families: GH-22 through GH-25 and GH-73 [6,7]. Family GH-73 proteins include *N*-acetylglucosaminidase, the bacterial flagellar protein (FlgJ), and autolysin [11,12]. *Salmonella enterica* FlgJ has N- and C-terminal domains crucial for rod assembly and peptidoglycan hydrolysis, respectively [11,13]. Although the structural and functional relationship of family GH-22 through GH-25 lysozymes has been well studied [5], little information is available on the structural features of family GH-73 enzymes. Recently, a crystallization paper describing the C-terminal domain of *S. enterica* FlgJ has been published [14].

The gram-negative bacterium *Sphingomonas* sp. strain A1 forms a huge pit on the cell surface through rearrangement of pleat molecules in the presence of the polysaccharide alginate [15]. This pit functions as a concentrator for extracellular alginate, and the polysaccharide is directly incorporated into the cytoplasm by an ABC transporter [8,16]. Flagellin homologues expressed on the cell surface but not present on flagella filaments function as a receptor-like molecule for alginate [17]. Structural and mutant analysis of flagellin homologues suggests that an α-domain consisting of N- and C-terminal regions is responsible for alginate binding [18]. Although strain A1 forms no flagella, more than 20 flagella-related

☆ The nucleotide sequences reported in this paper have been submitted to the DDBJ/GenBank/EMBL Data Bank with accession Nos. AB477427 for SPH1045, AB477428 for SPH1787, and AB477429 for SPH1797. The atomic coordinates and structure factors (code 2ZYC) of SPH1045-C have been deposited in the RCSB Protein Data Bank.

* Corresponding author. Fax: +81 774 38 3767.
E-mail address: kmurata@kais.kyoto-u.ac.jp (K. Murata).

0006-291X/$ - see front matter © 2009 Elsevier Inc. All rights reserved.
doi:10.1016/j.bbrc.2009.01.186

proteins, including FlgJ, are encoded in the strain A1 genome [8]. Structural and functional analysis of these proteins may contribute to clarification of the peculiar localization of flagellin homologues on the cell surface.

This article reports the first structural determination of family GH-73 peptidoglycan hydrolase, the C-terminal domain of FlgJ, by conducting X-ray crystallography.

Materials and methods

Microorganisms and culture conditions. *Escherichia coli* strain BL21(DE3) (Novagen) was used as the host for the expression of strain A1 FlgJ (SPH1045) and of its truncated form (SPH1045-C). For expression in *E. coli*, cells were aerobically pre-cultured at 30 °C in Luria-Bertani (LB) medium [19] supplemented with ampicillin (0.1 mg/ml). When the turbidity reached about 0.5 at 600 nm, isopropyl-β-D-thiogalactopyranoside was added to the culture (0.1 mM), and the cells were further cultured at 16 °C for 44 h.

Construction of the overexpression system. An overexpression system for the truncated SPH1045 (SPH1045-C), corresponding to the C-terminal domain of FlgJ, was constructed in *E. coli* cells as follows. To introduce the SPH1045-C gene into the pET21d vector (Novagen), polymerase chain reaction (PCR) was performed using KOD polymerase (Toyobo), with the strain A1 genomic DNA as the template and two synthetic oligonucleotides as primers. The oligonucleotides for SPH1045-C were 5′-GGCCATGGCACAGGCGTT CGTTGACGCAAC-3′ and 5′-GGCTCGAGGCCGCGCGCGGATGCGG CCGA-3′, with *Nco*I and *Xho*I sites (indicated by underlines) added to their 5′ regions, respectively. The pET21d vector is designed to express proteins with a hexahistidine (His_6)-tagged sequence at the C-terminus. The amplified truncated gene fragment was digested with *Nco*I and *Xho*I and then ligated with *Nco*I- and *Xho*I-digested pET21d. The entire SPH1045 gene fragment was also amplified by PCR (primers, 5′-GGCCATGATTGCGCGCCGAGCTGG AAG-3′ and 5′-CCCTCGAGGCCGCGCGCGGATGCGGCCGA-3′). The resultant gene was digested with *Nco*I and *Xho*I and ligated with *Nco*I- and *Xho*I-digested pET21d (Novagen). The resultant plasmids containing the entire and truncated genes were designated pET21d-SPH1045 and pET21d-SPH1045-C, respectively.

Purification. Unless otherwise specified, all operations were carried out at 0–4 °C. *E. coli* cells harboring pET21d-SPH1045-C were grown in 3.0 l of LB medium (1.5 l/flask), collected by centrifugation at 6000*g* and 4 °C for 5 min, washed with 20 mM Tris–HCl (pH 7.5), and then resuspended in the same buffer. The cells were ultrasonically disrupted (Insonator Model 201 M, Kubota) at 0 °C and 9 kHz for 20 min, and the clear solution obtained by centrifugation at 20,000*g* and 4 °C for 20 min was used as the cell extract. SPH1045-C was purified from the cell extract by affinity chromatography [Nickel ion-bound Chelating Sepharose (GE Healthcare, 1.5 × 5 cm)], followed by gel filtration chromatography [Sephacryl S-200HR (GE Healthcare, 2.6 × 65 cm)], and finally by cation-exchange chromatography [CM-Toyopearl 650M (Tosoh, 2.6 × 9.5 cm)]. The active fractions were combined and dialyzed against 20 mM Tris–HCl (pH 7.5). The dialysate was concentrated to about 25 mg/ml by ultrafiltration by using a Centriprep (M.W. cut-off, 10 kDa) (Millipore). The concentrate was used as the purified SPH1045-C. The purification procedure of the entire SPH1045 was almost the same as that of SPH1045-C.

Zymogram. Purified proteins (SPH1045 and SPH1045-C) were subjected to sodium dodecyl sulfate–polyacrylamide gel electrophoresis (SDS–PAGE) [20] containing *Micrococcus luteus* cells (Seikagaku Kogyo) in the gel. After electrophoresis, the gel was washed with potassium phosphate (pH 6.2) containing 1% Triton X-100 for renaturation, and the gel was then stained with 1% methylene blue in 0.01% KOH followed by destaining with distilled water, according to the methods reported in the literature [11].

Protein and enzyme assay. The protein content was determined using the method of Bradford [21], with bovine serum albumin as the standard. Unless otherwise described, bacteriolytic activity was assayed as follows: 5 μl of SPH1045-C (0.25 mg/ml) was added to 1 ml of *M. luteus* cell suspension in 50 mM Bis–Tris (pH 6.0). Transmittance at 540 nm was monitored at 25 °C on a Hitachi U-2001 spectrophotometer against a water blank. Initial velocity was obtained from the increase curve of transmittance.

Optimal pH and temperature and thermal stability. Experiments were carried out at 25 °C by using *M. luteus* cells as the substrate and purified SPH1045-C. Optimal pH: Reactions were performed at 25 °C in the following 50 mM buffers: sodium acetate, Bis–Tris, potassium phosphate, and Tris–HCl. Optimal temperature: Reactions were performed at various temperatures in 50 mM Bis–Tris (pH 6.0). Thermal stability: After preincubation of the enzyme at various temperatures for 10 min, residual activity was measured at 25 °C in 50 mM Bis–Tris (pH 6.0).

Crystallization and X-ray diffraction. SPH1045-C (25 mg/ml) was crystallized at 20 °C with the sitting-drop vapor-diffusion method. The mother liquor [1.0 M ammonium phosphate and 0.1 M Tris–HCl (pH 8.5)] (100 μl) was used as a reservoir solution, and 1 μl of SPH1045-C was mixed with 1 μl of the reservoir solution to form the drop. An enzyme crystal was soaked in the mother liquor containing 20% glycerol for cryoprotection. The crystal was removed from the soaking solution by using a mounted nylon loop (Hampton Research) and then placed directly into a cold nitrogen gas stream at −173 °C. To obtain a derivative for phasing, the native crystal was soaked at 20 °C for 3 h in the mother liquor containing 20 mM K_2AuCl_4. X-ray diffraction images were collected from the native crystal at −173 °C under a nitrogen gas stream by using a

Table 1
Data collection and refinement statistics.

	Native (SPH1045-C)	Derivative (SPH1045-C/Au)
Data collection		
Wavelength (Å)	1.0000	1.0395
Space group	$P4_32_12$	$P4_12_12$
Unit cell parameters (Å)	$a = b = 54.3$, $c = 102.8$	$a = b = 54.8$, $c = 104.5$
Resolution limit (Å)	30.0–1.74 (1.80–1.74)[a]	50.0–1.90 (1.97–1.90)
Total reflections	177,801	283,020
Unique reflections	16,510	13,202
Redundancy	10.8 (9.9)	12.0 (11.9)
Completeness (%)	100.0 (99.9)	97.9 (97.0)
I/Sigma (I)	14.6 (4.28)	14.2 (7.06)
R_{merge} (%)	5.5 (39.6)	6.1 (37.4)
Refinement		
Final model	155 residues, 184 water molecules, 1 phosphate ion	
Resolution limit (Å)	30.0–1.74 (1.79–1.74)	
Used reflections	15,603 (1,114)	
Completeness (%)	99.9 (99.9)	
R-factor (%)	19.9 (24.8)	
R_{free} (%)	23.8 (36.1)	
Average *B*-factor (Å^2)		
Protein	18.4	
Waters	31.8	
Phosphate ion	26.2	
Root mean square deviations		
Bond (Å)	0.008	
Angle (°)	1.02	
Ramachandran plot (%)		
Most favored regions	95.5	
Additional allowed regions	4.5	
Generously allowed regions	0.0	

[a] Data on the highest shells are given in parentheses.

Jupiter210 detector and synchrotron radiation at the BL-38B1 station of SPring-8 (Japan). The diffraction data for the native crystal were obtained to 1.74 Å resolution and processed using the *HKL2000* program package [22]. Single-wavelength anomalous diffraction (SAD) data were collected from the crystal derived with Au and processed at a redundancy of 12.0 with each Friedel pair. Data collection statistics from the native and derivative crystals are summarized in Table 1.

Structure determination and refinement. The crystal structure of SPH1045-C was resolved by SAD by using the Au derivative crystal. Au sites were determined using the *SHELXD* program [23]. Initial phasing, density modification, and automatic model building were conducted using the *SHELXE* [24] and *ARP/wARP* programs [25] in the CCP4 program package [26]. The *Coot* program [27] was used for manual modification of the initial model. The 30.0–1.74 Å resolution dataset was truncated using the CCP4 program package and used for subsequent refinement. Initial rigid-body refinement and several rounds of restrained refinement against the dataset were conducted using the *Refmac5* program [28]. Water molecules were incorporated when the difference in density exceeded 3.0 σ above the mean, and when the $2F_o - F_c$ map showed a density of over 1.0 σ. Refinement continued until convergence at 1.74 Å resolution. Protein models were superimposed and their root-mean-square-deviations (RMSD) were determined using the *LSQKAB* program [29], a part of CCP4. Final model quality was checked using the *PROCHECK* program [30]. Ribbon plots were prepared using the *PyMOL* program [31]. Coordinates used in this paper were taken from the RCSB Protein Data Bank (PDB) [32].

Results and discussion

Sphingomonas sp. strain A1 proteins similar to family GH-73 FlgJ

In order to determine strain A1 proteins homologous to *S. enterica* FlgJ, the *PSI-BLAST* program (http://psiblast.ddbj.nig.ac.jp/top-j.html) was used to search for sequence similarity against the strain A1 genome database [8]. Three strain A1 hypothetical proteins [SPH1045 (33.4 kDa), SPH1787 (12.6 kDa), and SPH1797 (26.0 kDa)] showed a significant identity with *S. enterica* FlgJ (UniProt ID, Q8Z7K1). SPH1045 versus FlgJ showed a 41.1% identity in a 282 amino acid overlap; SPH1787 versus FlgJ showed a 38.7% identity in an 88 amino acid overlap; and SPH1797 versus FlgJ showed a 41.9% identity in a 172 amino acid overlap. Both SPH1045 and SPH1797 contain two regions corresponding to the N- and C-terminal domains of FlgJ, although only the N-terminal domain is included in SPH1787 (Fig. 1). Two acid residues (Glu223 and Asp248) in the C-terminal domain of FlgJ are important for peptidoglycan hydrolysis [11]. These two residues are completely conserved in SPH1045 and SPH1797. Since SPH1045, having a peptidoglycan hydrolase domain, exhibits a high identity with FlgJ throughout the entire sequence, hereafter we focus on SPH1045, especially the C-terminal domain (residues 152–313) corresponding to peptidoglycan hydrolase [SPH1045-C (18 kDa)] (Fig. 1).

Enzyme characteristics

In order to examine whether SPH1045 and SPH1045-C show peptidoglycan hydrolase activity, both proteins expressed in *E. coli* cells were purified and subjected to Zymogram analysis. A clear zone corresponding to each protein band (SPH1045, 33 kDa and SPH1045-C, 17 kDa) was observed on the renatured and methylene blue-stained SDS–PAGE gel (data not shown), indicating that both proteins exhibit bacterial cell lysis activity. Thus, the enzyme activity was determined by measuring the increase in transmittance at 540 nm. Enzyme properties of the purified SPH1045-C are discussed below.

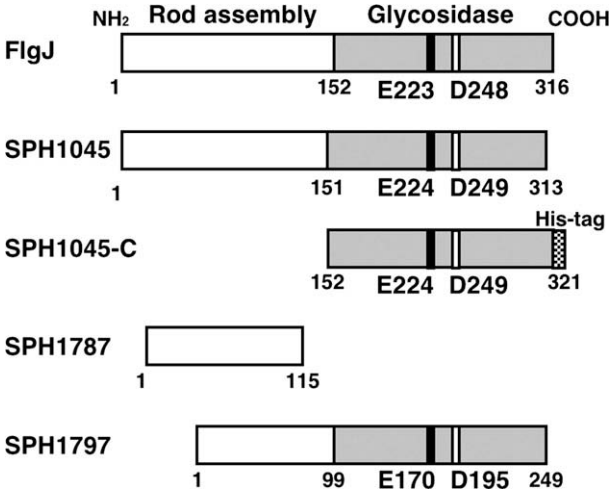

Fig. 1. Schematic diagram of strain A1 proteins similar to *Salmonella* FlgJ.

Molecular mass. The molecular mass of SPH1045-C, including the His-tagged sequence at the C-terminus, was determined to be 18 kDa by SDS–PAGE (Fig. S1A). This was near to the theoretical value (18,699 Da) deduced from the predicted amino acid sequence of the enzyme. On permeation chromatography using Sephacryl S-200HR, the enzyme was eluted as a protein with a molecular mass of about 17 kDa (Fig. S1B), indicating that the enzyme is monomeric.

pH and temperature. SPH1045-C was most active at pH 6.0 in 50 mM Bis–Tris (Fig. S2A) and at 37 °C (Fig. S2B). More than 50% of the enzyme activity remained after boiling for 10 min in 50 mM Tris–HCl (pH 7.5) (Fig. S2C), indicating that the enzyme is thermostable.

Effect of chemicals. The effects of different chemicals on enzyme activity were examined (Table S1). Metal ions, including Al^{3+}, Cu^{2+}, Fe^{3+}, Fe^{2+}, Hg^{2+}, and Zn^{2+}, significantly inhibited enzyme activity. Chelators (EDTA and EGTA) at 1 mM, thiol reagents at 1 mM (dithiothreitol, reduced glutathione, and 2-mercaptoethanol), and sugars at 5 mM (D-galactose, D-glucose, and D-glucuronic acid) had no significant effect on enzyme activity.

Structure determination

Angular crystals of SPH1045-C were found in a droplet consisting of 1.0 M ammonium phosphate and 0.1 M Tris–HCl (pH 8.5) (Fig. S1C). Diffraction images were collected at up to 1.74 Å resolution from the crystal. For phasing by SAD analysis, diffraction images were collected from the Au-derivative crystal. Data collection statistics are shown in Table 1. The refined model includes 155 amino acid residues, 184 water molecules, and 1 phosphate ion for every molecule of SPH1045-C. All amino acid residues (Ala153–Gly313), except for Glu224–Arg230 and the C-terminal His-tagged sequence (His316–His321), could be assigned in the $2F_o - F_c$ map. Refinement statistics are summarized in Table 1.

Overall structure

The overall structure (Fig. 2A) and topology of secondary structure elements (Fig. 2B) indicate that SPH1045-C consists of an α-barrel lobe composed of the N- and C-terminal domains and a β-sheet lobe in the center region. The α-lobe consists of seven α-helices (H1, residues 154–171; H2, 175–186; H3, 243–256; H4, 258–260; H5, 269–278; H6, 287–296; H7, 298–307). The β-lobe includes long

loops and an antiparallel β-sheet composed of two β-strands (S1, 216–222; S2, 233–239). A deep cleft is located between the two lobes. The cleft is sufficiently large to accommodate a peptide loop of a neighboring molecule in the crystal packing (Fig. 2C).

Structural homologues of the GH-73 family SPH1045-C were searched for in the PDB by using the *DALI* program [33]. Several proteins with α and β lobes as a basic scaffold were found to exhibit a slight structural homology with SPH1045-C (Table S2). The overall structure of SPH1045-C is most similar to that of the peptidoglycan-degrading enzyme from bacteriophage ψ 29 (PDB ID, 3csq, $Z = 6.8$) with an RMSD of 3.8 Å for 121 C^{α}. SPH1045-C is also structurally similar to family GH-22 and GH-23 lysozymes ($Z = 5$–6). Superimposition of the crystal structures of SPH1045-C and family GH-23 lysozymes (PDB ID, 153l) is shown in Fig. 3A. A large number of lysozymes with α and β lobes are categorized into a "lysozyme-like" fold on the SCOP database (http://scop.mrc-lmb.cam.ac.uk/scop/). Although SPH1045 is classified into family GH-73, which is distinct from lysozyme GH families based on the primary structure, GH-73 enzymes will be structurally classified into this fold.

Active site

In the case of family GH-22 and GH-23 lysozymes, a cleft located between the two lobes includes the active site. The deep cleft is also found between the two lobes in SPH1045-C, suggesting that the substrate peptidoglycan is bound to this active cleft. Glu223 and Asp248 of *Salmonella* FlgJ are thought to function as catalytic residues by site-directed mutagenesis [11]. SPH1045-C Asp249 corresponding to FlgJ Asp248 is, however, located far from the active cleft (Fig. 3B), suggesting that this residue should be re-estimated regarding catalysis through structural analysis of the substrate-bound enzyme. Although SPH1045-C Glu224 could not be assigned in the $2F_o - F_c$ map, this residue is probably located near the active site (Fig. 3B).

Despite a similarity in the overall structure, there is a difference in the arrangement of a catalytically important residue in the active site among family GH-22, GH-23, and GH-73 enzymes. Glu35 and Asp52(53) in family GH-22 lysozymes are regarded as the proton donor and the nucleophile/base, respectively [34,35]. The catalytic glutamate residues acting as the proton donors are well superimposed in family GH-22 (Glu35), GH-23 (Glu74), and GH-73 (Glu185) enzymes (Fig. 3C and D), but there is no structural similarity around the nucleophile/base Asp residue (Fig. 3C and D). Asp97 in family GH-23 seems to correspond to Asp53 in family GH-22. Asp97 has recently been suggested to be crucial for the catalytic reaction [35]. In the case of SPH1045-C, Lys208 is positionally comparable with family GH-22 Asp53 (Fig. 3B and C). Further analysis is essential to clarify the catalytic reaction mechanisms of family GH-73 enzymes.

In conclusion, most peptidoglycan hydrolases, including lysozymes, share the common basic scaffold (α and β lobes) and proton donor residues (Glu), but the arrangement of the nucleophile/base residue is specific to each GH family.

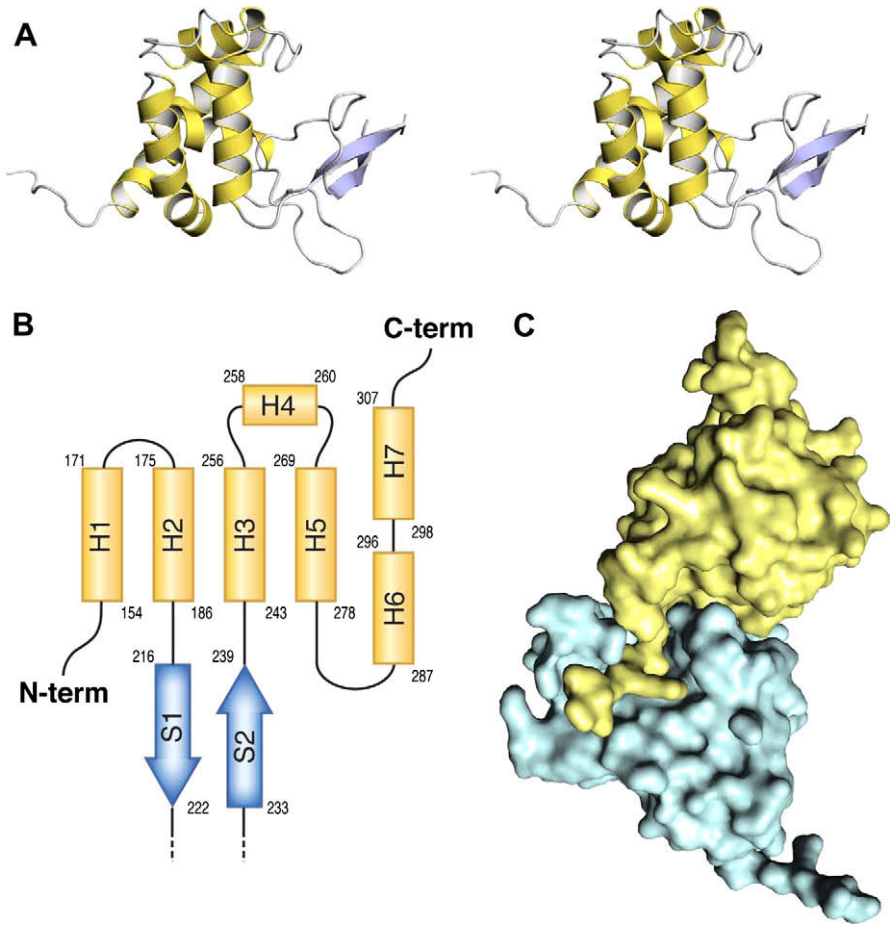

Fig. 2. Structure of SPH1045-C. (A) Overall structure (stereodiagram). (B) Topology diagram. α-Helices are shown as yellow cylinders and β-strands are as blue arrows. (C) Crystal packing. A molecule (yellow) is bound to the active cleft of the neighboring molecule (blue).

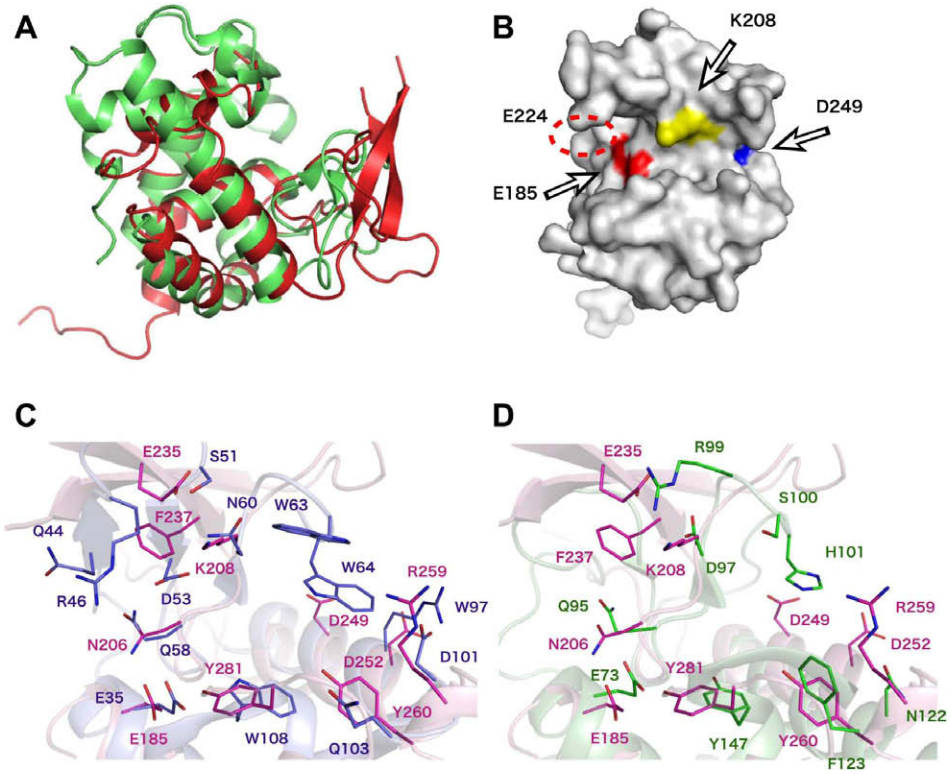

Fig. 3. Structural comparison. (A) Superimposition of the overall structures of SPH1045-C (red) and family GH-23 lysozymes (green) (PDB ID, 153l). (B) Molecular surface model of SPH1045-C. The possible proton donor (Glu185) is colored red. The catalytically important Asp249 indicated by using site-directed mutagenesis [11] is colored blue. (C) Superimposition of the active sites of SPH1045-C (purple) and family GH-22 lysozymes (blue) (PDB ID, 2z2e). (D) Superimposition of the active sites of SPH1045-C (purple) and family GH-23 lysozymes (green) (PDB ID, 153l).

Acknowledgments

We thank Drs. K. Hasegawa and S. Baba of the Japan Synchrotron Radiation Research Institute (JASRI) for their kind help in data collection. Diffraction data for crystals were collected at the BL-38B1 station of SPring-8 (Japan) with the approval of JASRI. This work was supported in part by Targeted Proteins Research Program from the Ministry of Education, Culture, Sports, Science, and Technology (MEXT) of Japan. Part of this work was supported by Showa Houkoukai Foundation.

Appendix A. Supplementary data

Supplementary data associated with this article can be found, in the online version, at doi:10.1016/j.bbrc.2009.01.186.

References

[1] N. Nanninga, Morphogenesis of *Escherichia coli*, Microbiol. Mol. Biol. Rev. 62 (1998) 110–129.
[2] W. Vollmer, D. Blanot, M.A. de Pedro, Peptidoglycan structure and architecture, FEMS Microbiol. Rev. 32 (2008) 149–167.
[3] G.D. Shockman, L. Daneo-Moore, R. Kariyama, O. Massidda, Bacterial walls, peptidoglycan hydrolases, autolysins, and autolysis, Microb. Drug Resist. 2 (1996) 95–98.
[4] W. Vollmer, B. Joris, P. Charlier, S. Foster, Bacterial peptidoglycan (murein) hydrolases, FEMS Microbiol. Rev. 32 (2008) 259–286.
[5] A.F. Monzingo, E.M. Marcotte, P.J. Hart, J.D. Robertus, Chitinases, chitosanases, and lysozymes can be divided into prokaryotic and eukaryotic families sharing a conserved core, Nat. Struct. Biol. 3 (1996) 133–140.
[6] G.J. Davies, T.M. Gloster, B. Henrissat, Recent structural insights into the expanding world of carbohydrate-active enzymes, Curr. Opin. Struct. Biol. 15 (2005) 637–645.
[7] B.L. Cantarel, P.M. Coutinho, C. Rancurel, T. Bernard, V. Lombard, B. Henrissat, The Carbohydrate-Active EnZymes database (CAZy): an expert resource for Glycogenomics, Nucleic Acids Res. 37 (2009) D233–238.
[8] K. Murata, S. Kawai, B. Mikami, W. Hashimoto, Superchannel of bacteria: biological significance and new horizons, Biosci. Biotechnol. Biochem. 72 (2008) 265–277.
[9] Z. Cui, Y. Maruyama, B. Mikami, W. Hashimoto, K. Murata, Crystal structure of glycoside hydrolase family 78 α-L-rhamnosidase from *Bacillus* sp. GL1, J. Mol. Biol. 374 (2007) 384–398.
[10] A. Ochiai, T. Itoh, Y. Maruyama, A. Kawamata, B. Mikami, W. Hashimoto, K. Murata, A novel structural fold in polysaccharide lyases: *Bacillus subtilis* family 11 rhamnogalacturonan lyase YesW with an eight-bladed β-propeller, J. Biol. Chem. 282 (2007) 37134–37145.
[11] T. Nambu, T. Minamino, R.M. Macnab, K. Kutsukake, Peptidoglycan-hydrolyzing activity of the FlgJ protein, essential for flagellar rod formation in *Salmonella typhimurium*, J. Bacteriol. 181 (1999) 1555–1561.
[12] G.J. Horsburgh, A. Atrih, M.P. Williamson, S.J. Foster, LytG of *Bacillus subtilis* is a novel peptidoglycan hydrolase: the major active glucosaminidase, Biochemistry 42 (2003) 257–264.
[13] T. Hirano, T. Minamino, R.M. Macnab, The role in flagellar rod assembly of the N-terminal domain of *Salmonella* FlgJ, a flagellum-specific muramidase, J. Mol. Biol. 312 (2001) 359–369.
[14] Y. Kikuchi, H. Matsunami, M. Yamane, K. Imada, K. Namba, Crystallization and preliminary X-ray analysis of a C-terminal fragment of FlgJ-a putative flagellar rod cap protein from *Salmonella*, Acta Crystallogr. Sect. F Struct. Biol. Cryst. Commun. 65 (2009) 17–20.
[15] T. Hisano, N. Kimura, W. Hashimoto, K. Murata, Pit structure on bacterial cell surface, Biochem. Biophys. Res. Commun. 220 (1996) 979–982.
[16] J. He, H. Nankai, W. Hashimoto, K. Murata, Molecular identification and characterization of an alginate-binding protein on the cell surface of *Sphingomonas* sp. A1, Biochem. Biophys. Res. Commun. 322 (2004) 712–717.
[17] W. Hashimoto, J. He, Y. Wada, H. Nankai, B. Mikami, K. Murata, Proteomics-based identification of outer-membrane proteins responsible for import of macromolecules in *Sphingomonas* sp. A1: alginate-binding flagellin on the cell surface, Biochemistry 44 (2005) 13783–13794.
[18] Y. Maruyama, M. Momma, B. Mikami, W. Hashimoto, K. Murata, Crystal structure of a novel bacterial cell-surface flagellin binding to a polysaccharide, Biochemistry 47 (2008) 1393–13402.
[19] J. Sambrook, E.F. Fritsch, T. Maniatis, Molecular Cloning, A Laboratory Manual, second ed., Cold Spring Harbor Laboratory Press, Cold Spring Harbor, NY, 1989.
[20] U.K. Laemmli, Cleavage of structural proteins during the assembly of the head of bacteriophage T4, Nature 227 (1970) 680–685.
[21] M.M. Bradford, A rapid and sensitive method for the quantification of microgram quantities of protein utilizing the principle of protein-dye binding, Anal. Biochem. 72 (1976) 248–254.

[22] Z. Otwinoski, W. Minor, Processing of X-ray diffraction data collected in oscillation mode, Methods Enzymol. 276 (1997) 307–326.
[23] T.R. Schneider, G.M. Sheldrick, Substructure solution with SHELXD, Acta Crystallogr. D58 (2002) 1772–1779.
[24] G.M. Sheldrick, Macromolecular phasing with SHELXE, Z. Kristallogr. 217 (2002) 644–650.
[25] A. Perrakis, R. Morris, V.S. Lamzin, Automated protein model building combined with iterative structure refinement, Nat. Struct. Biol. 6 (1999) 458–463.
[26] Collaborative Computational Project, The CCP4 suite: programs for protein crystallography, Acta Crystallogr. D50 (1994) 760–763.
[27] P. Emsley, K. Cowtan, Coot: model-building tools for molecular graphics, Acta Crystallogr. D60 (2004) 2126–2132.
[28] G.N. Murshudov, A.A. Vagin, E.J. Dodson, Refinement of macromolecular structures by the maximum-likelihood method, Acta Crystallogr. D53 (1997) 240–255.
[29] W. Kabsch, A solution for the best rotation to relate two sets of vectors, Acta Crystallogr. A32 (1976) 922–923.
[30] R.A. Laskowski, M.W. MacArthur, D.S. Moss, J.M. Thornton, PROCHECK: a program to check the stereochemical quality of protein structures, J. Appl. Crystallogr. 26 (1993) 283–291.
[31] W.L. DeLano, on World Wide Web http://www.pymol.org (2002).
[32] H.M. Berman, J. Westbrook, Z. Feng, G. Gilliland, T.N. Bhat, H. Weissig, I.N. Shindyalov, P.E. Bourne, The Protein Data Bank, Nucleic Acids Res. 28 (2000) 235–242.
[33] L. Holm, C. Sander, Protein structure comparison by alignment of distance matrices, J. Mol. Biol. 233 (1993) 123–138.
[34] N.C. Strynadka, M.N. James, Lysozyme: a model enzyme in protein crystallography, EXS 75 (1996) 185–222.
[35] H. Hirakawa, A. Ochi, Y. Kawahara, S. Kawamura, T. Torikata, S. Kuhara, Catalytic reaction mechanism of goose egg-white lysozyme by molecular modeling of enzyme-substrate complex, J. Biochem. 144 (2008) 753–761.